

Survival probability time distribution in dielectric cavities

Jung-Wan Ryu^{1,2}, Soo-Young Lee¹, Chil-Min Kim¹, and Young-Jai Park²

¹ National Creative Research Initiative Center for Controlling Optical Chaos,
Pai-Chai University, Daejeon 302-735, Korea and

² Department of Physics, Sogang University, Seoul 121-742, Korea

We study the survival probability time distribution (SPTD) in dielectric cavities. In a circular dielectric cavity the SPTD has an algebraic long time behavior, $\sim t^{-2}$ in both TM and TE cases, but shows different short time behaviors due to the existence of the Brewster angle in TE case where the short time behavior is exponential. The SPTD for a stadium-shaped cavity decays exponentially, and the exponent shows a relation of $\gamma \sim n^{-2}$, n is the refractive index, and the proportional coefficient is obtained from a simple model of the steady probability distribution. We also discuss about the SPTD for a quadrupolar deformed cavity and show that the long time behavior can be algebraic or exponential depending on the location of islands.

PACS numbers: 05.60.Cd, 42.15.-i, 05.45.-a

I. INTRODUCTION

Recently, lasing modes from dielectric microcavities have attracted much attention due to its potential application to optoelectric circuits and optical communications [1]. In particular, there was a lot of theoretical and experimental effort to excite directional lasing modes in deformed microcavities [2]. It is now well known that the lasing pattern has a very close relationship with the internal ray dynamics given by the boundary geometry of cavity. It is also reported that the property of the openness of the dielectric cavity plays an important role in the resonance pattern analysis [3, 4].

For a general open system, the survival probability time distribution (SPTD) or its time derivative, the escape time distribution, is a basic physical quantity. Many studies are focused on the relation between the long time behavior of the SPTD and the internal dynamics, and it is known that the SPTD has algebraic and exponential decays in integrable and chaotic systems, respectively [5, 6, 7, 8, 9, 10]. In mixed systems, having both integrable islands and chaotic sea in phase space, the SPTD has algebraic long time behavior which originates from the slow escape mechanism due to the stickiness of KAM tori [11].

The property of openness of the dielectric cavity is different from the open systems previously studied [5, 6, 7, 8, 9, 10]. Rays can escape through any boundary point, and partial escapes, depending on the incident angle, are possible. This unique property can be reflected on the long time behavior of the SPTD.

In this paper, we study the SPTD in dielectric cavities of various boundary geometries such as circle, stadium, and quadrupole, which are typical examples of integrable, chaotic, and mixed systems, respectively. The SPTDs in these dielectric cavities show basically similar behavior to the open cavity with a small hole on the cavity boundary, but the exponents are different. In particular, we show that the ergodic property cannot be applied for the stadium-shaped dielectric cavity even in the small opening limit, $n \rightarrow \infty$, n is the refractive index.

The paper is organized as follows. In Sec. II the algebraic long time behavior of the SPTD in the circular dielectric cavity is derived analytically and confirmed numerically for both TM and TE waves. It is shown in Sec. III that the SPTD for a stadium-shaped cavity decays exponentially, and the exponent γ has $\sim n^{-2}$ dependence and the proportional coefficient can be understood from a simple model of the steady probability distribution (SPD). The SPTD in the quadrupole-deformed dielectric cavity is discussed in Sec. IV and we finally summarize the results in Sec. V.

II. CIRCULAR DIELECTRIC CAVITY - INTEGRABLE SYSTEM

Many authors have studied the SPTD for the open billiard with a small hole on boundary [5, 6, 7, 8]. It is known that the SPTD in a circular billiard decays algebraically, $P_{sv}(t) \propto t^{-1}$. In this section we study the SPTD for the circular dielectric cavity, and it will be shown that the SPTD shows still an algebraic decay but the exponent is different.

For simplicity, we focus on TM wave first and for TE wave we will mention only difference later. In the circular geometry, ray dynamics is integrable and rays in the open area of the phase space, i.e., $-1/n < p < 1/n$, $p = \sin \theta$, θ being the incident angle, can partially escape from the cavity. The formal expression of the SPTD in the circular dielectric cavity is given by

$$P_{sv}(t) = \frac{n}{2L} \int_0^L ds \int_{-p_c}^{p_c} dp R(p)^{N(t)}, \quad (1)$$

where L is the boundary length, and p_c is the critical line for total internal reflection, i.e., $p_c = \sin \theta_c = 1/n$, and $R(p)$ is the reflection coefficient for TM wave [12],

$$R(\theta) = \left(\frac{n \cos \theta - \cos \theta_t}{n \cos \theta + \cos \theta_t} \right)^2, \quad (2)$$

where $n \sin \theta = \sin \theta_t$, and $N(t)$ is the number of bounce on the boundary. Since $N(t) = t/2 \cos \theta$ in the circular geometry, when considering a unit circle and a time scale as the length of ray trajectory, Eq.(1) can be rewritten as

$$P_{sv}(t) = n \int_0^{\theta_c} d\theta \cos \theta \exp[-G(\theta)t], \quad (3)$$

where

$$G(\theta) \equiv \frac{1}{\cos \theta} \ln \left(1 + \frac{2 \cos \theta_t}{n \cos \theta - \cos \theta_t} \right). \quad (4)$$

Note that the rays near the critical line p_c can survive longer time and dominate long time tail behavior. Therefore, we can expand $G(\theta)$ from θ_c by changing variable, $\theta = \theta_c - \chi$, as

$$G(\theta) \approx \alpha \chi^{1/2} + \beta \chi^{3/2} + \dots, \quad (5)$$

where

$$\alpha = \frac{2n\sqrt{2\sqrt{n^2-1}}}{n^2-1} \quad (6)$$

and

$$\beta = -\alpha \left(\frac{n^2-6}{4\sqrt{n^2-1}} - \frac{2}{n} \right). \quad (7)$$

Substituting the lowest term in Eq.(5) into Eq.(3), we can obtain the long time behavior of the SPTD as

$$\begin{aligned} P_{sv}(t) &\simeq \frac{2\sqrt{n^2-1}}{\alpha^2} t^{-2} \left[1 - (1 + \alpha\sqrt{\theta_c t}) e^{-\alpha\sqrt{\theta_c t}} \right] \\ &\simeq \frac{2\sqrt{n^2-1}}{\alpha^2} t^{-2}. \end{aligned} \quad (8)$$

We emphasize that the SPTD for the circular dielectric cavity decays as t^{-2} as shown in Eq.(8), different from the open billiard with a small hole where decays as t^{-1} . This means that the property of openness can change the exponent of the algebraic decaying SPTD.

For TE wave case the reflection coefficient is given by

$$R_{TE}(\theta) = \left(\frac{n \cos \theta_t - \cos \theta}{n \cos \theta_t + \cos \theta} \right)^2, \quad (9)$$

and the expansion of $G(\theta)$ and the SPTD at a long time are the same as Eq.(5) and Eq.(8) with different expansion coefficients, i.e.,

$$\alpha_{TE} = \frac{2n^3\sqrt{2\sqrt{n^2-1}}}{n^2-1} = n^2\alpha \quad (10)$$

and

$$\beta_{TE} = -\frac{\alpha_{TE}}{4\sqrt{n^2-1}}(8n^4 + n^2 + 6). \quad (11)$$

We note that the dependence of the SPTD on the refractive index n in TM and TE waves is quite different, i.e.,

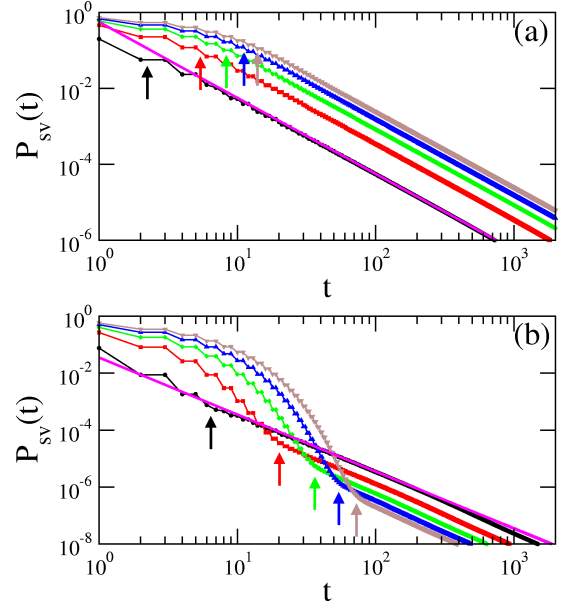


FIG. 1: (color online) The SPTDs of the circular dielectric cavity for (a) TM and (b) TE waves. Black circle, red square, green diamond, blue triangle (up), and brown triangle (down) are for $n=2, 4, 6, 8,$ and $10,$ respectively. These shows t^{-2} long time behavior and a very good agreement with the solid lines which represent the $n = 2$ case in Eq.(8).

$P_{sv}(t) \simeq n^2 t^{-2}$ for TM case, but $P_{sv}(t) \simeq n^{-2} t^{-2}$ for TE case. The proportionality of n^{-2} of the TE case does not mean that the circular cavity with a higher n is more leaky, since we take into account of only the open region in the phase space, $-1/n < p < 1/n$ (see Eq.(1)).

In order to perform numerical calculation for the SPTD in the circular cavity, we take 10^8 random initial points in the open region of the phase space. We then trace each point with a weight determined by $R(p)$ when bouncing from the boundary, and sum the weights between t and $t + \Delta$, we take $\Delta = 1$ in the calculations, for all points in the ensemble, and finally normalize to be unit when $t = 0$. Figure 1 shows the numerical results of the SPTD in the circular cavity for TM and TE cases. It is clear that the SPTD for both cases shows an algebraic long time behavior, $\sim t^{-2}$, and the dependence on n is correctly described by Eq.(8) which is indicated by the solid lines for $n = 2$ in Fig.1.

A substantial difference between the TM and TE cases appears in the short time behavior. As shown in Fig. 1 (a) the short time behavior of the TM SPTD is smoothly connected to the t^{-2} long time tail, on the other hand that of the TE SPTD shows rather an abrupt transition to the algebraic long time tail and the detail of the short time behavior seems to be characterized by an exponential decay. This exponential short time decay is clear in Fig. 2 (a) and the exponent $\gamma(n)$, when fitted as $\exp(-\gamma(n)t)$, appears as the solid dots in Fig. 2 (b). These exponents are well described by a simple approxi-

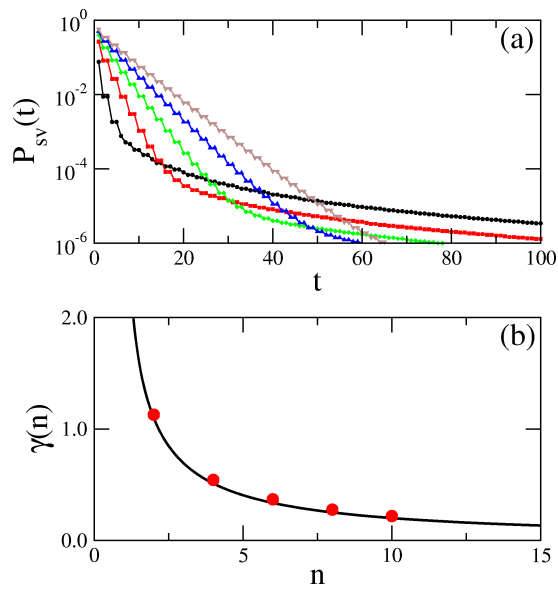


FIG. 2: (color online) (a) The exponential short time behavior of the SPTDs for TE case. The colors for different n is the same as in Fig. 1. These can be fitted as $\exp(-\gamma(n)t)$ in a short time range. (b) The exponents $\gamma(n)$. The solid line represents the result of a simple approximation of Eq.(13) .

mation for the reflection coefficient $R_{TE}(\theta)$. If we expand $R_{TE}(\theta)$ at $\theta = 0$ and take only the lowest term, then

$$P_{sv}(t) \simeq \exp\left(-\ln\left(\frac{n+1}{n-1}\right)t\right) = \exp(-\gamma(n)t). \quad (12)$$

The solid line in Fig. 2 (b) represents the relation

$$\gamma(n) = \ln\left(\frac{n+1}{n-1}\right). \quad (13)$$

Here we emphasize that although the lowest term of the expansion of Eq.(12) is the same for both TM and TE cases, only TE case allows the exponential short time decay. The reason for this is the existence of the Brewster angle in the TE case, $\theta_B = \arctan(1/n)$ where rays can escape without reflection, i.e., $R(\theta_B) = 0$. The rays with the incident angle in the range of $-\theta_B < \theta < \theta_B$ dominate the short time behavior, while the other parts, $\theta_B < |\theta| < \theta_c$, mainly contribute to the long time algebraic tail.

It is important to know when the algebraic decay starts to appear in both TM and TE cases. In TM case, the main factor for the deviation from the t^{-2} decay comes from the finite integral bound, and it corresponds to the terms containing the upper bound θ_c in Eq.(8). We then estimate the transition time when the deviation from the t^{-2} decay is about 10 %, and the result is

$$t_c \simeq \frac{1.38(n^2 - 1)^{3/4}}{n\sqrt{\arcsin(1/n)}} \propto n. \quad (14)$$

In Fig. 1 (a) the corresponding transition times are indicated by arrows and show a good agreement with the

numerical calculations for various n .

Due to the existence of the Brewster angle, the transition time for TE SPTD can be determined by a different way. As mentioned above, the TE SPTD shows a short time exponential behavior and a long time algebraic behavior. Therefore we can estimate the transition time by finding the intersection time for both different behaviors. From Eq.(8) with α_{TE} and Eq.(12), for a large n we can get an implicit equation for the transition time as

$$\frac{t_c}{n} \exp\left(-\frac{t_c}{n}\right) = \frac{1}{2n^2}. \quad (15)$$

The transition times for various refractive indices are indicated by arrows in Fig. 1 (b) and well represent the transition times of the numerical results. The solution t_c of the above equation cannot be described by a simple power of n , but we can show

$$t_c(n) \propto n^{\mu(n)}, \quad \mu(n) > 1. \quad (16)$$

If we take a logarithm of Eq.(15), then we get

$$\frac{t_c}{n} - \ln \frac{t_c}{n} = \ln 2n^2, \quad (17)$$

which generally has two solutions and the larger solution is relevant. The point t_0 , at which the slopes of the two functions in the left hand side of the above equation are identical, should locate between the two solutions. By differentiating the above equation, we get $t_0 = n$. Therefore,

$$t_c > t_0 = n. \quad (18)$$

Even though both TM and TE cases show the same t^{-2} long time decay in the circular cavity, the short time behavior and the n dependence of the transition time are quite different. We emphasize that these differences originate from the existence of the Brewster angle in the TE case.

III. STADIUM-SHAPED DIELECTRIC CAVITY - CHAOTIC SYSTEM

As an example of chaotic dielectric cavities, we take a stadium-shaped one with parallel linear segments of a length l and two semicircles of a radius R . The stadium-shaped billiard has been a typical chaotic system in the research of classical and quantum chaos. The escape property through a small hole on the boundary of the stadium-shaped billiard has been investigated by many authors [9]. They have shown that the escape time distribution exponentially decays first and later becomes algebraic, and the transition time t_c increases as the hole size decreases. The algebraic decay at long times comes from the stickiness near the marginally stable line in phase space corresponding to the bouncing ball trajectories. On the other hand, in the stadium-shaped dielectric cavity

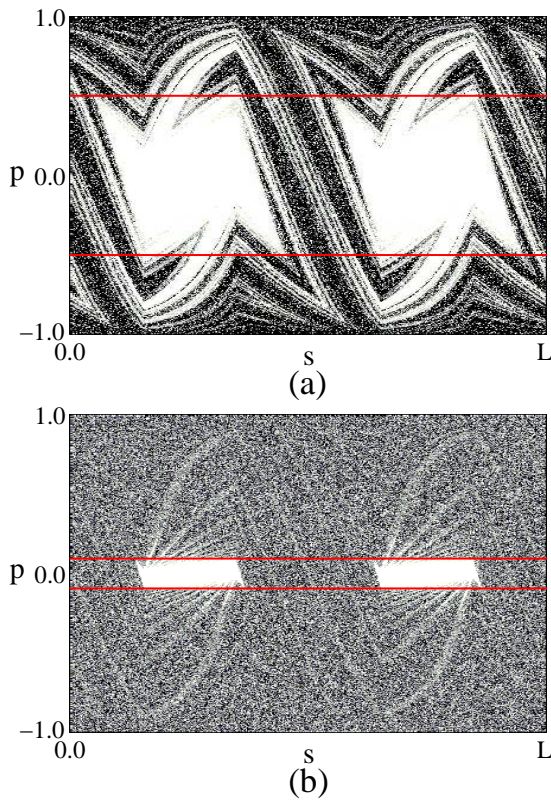


FIG. 3: The steady probability distributions. (a) $n = 2$ case with system parameters $(R, l) = (1, 2)$ for TM wave. (b) $n = 10$ case with system parameters $(R, l) = (1, 2)$ for TM wave. The black points indicate the rays traced from a random ensemble with weights higher than 0.1 at about $t = 12$ in $n = 2$ case and $t = 37$ in $n = 10$ case. The solid lines denote the critical line $\pm p_c$ for total internal reflection.

the ray trajectories of the bouncing ball type cannot contribute to the long time behavior due to the property of openness, i.e., rays with almost vertical incidence escape easily and contribute to the short time behavior. As a result the SPTD shows only exponential decay (see Fig. 4, 5).

The exponential decay in the dielectric chaotic cavity implies the existence of the *steady probability distribution* (SPD), $P_s(s, p)$ which is defined as the spatial part of the survival probability distribution $\tilde{P}_{sv}(s, p, t)$ [3]. With this SPD, we can express the SPTD as

$$P_{sv}(t) = \int_0^L ds \int_{-1}^1 dp \tilde{P}_{sv}(s, p, t) \simeq C \exp(-\gamma t), \quad (19)$$

where C is a constant and

$$\gamma = \int_0^L ds \int_{-1}^1 dp P_s(s, p) T(p), \quad (20)$$

where the transmission coefficient $T(p)$ is given as $T(p) = 1 - R(p)$.

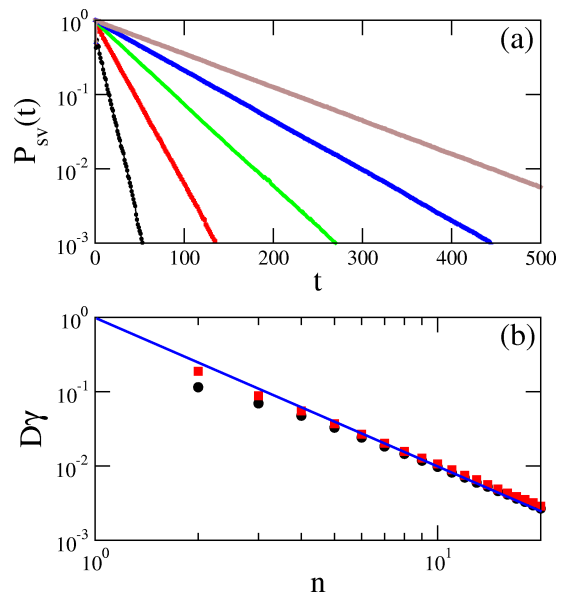


FIG. 4: (color online) The SPTD and the decay rates for TM wave. (a) The exponential SPTD for a stadium dielectric cavity with $(R, l) = (1, 1)$. Black, red, green, blue, and brown lines are for $n=2, 4, 6, 8,$ and 10 , respectively. (b) The decay rates with increasing n . Black circle and red square represent results for system parameters $(R, l) = (1, 1)$ and $(1, 2)$, respectively. The solid line shows n^{-2} behavior. The coefficient D is given as $D = \frac{\sqrt{AL}}{2\pi^2 R}$.

Note that the above equation is satisfied in the exponential decay region and cannot describe the nonexponential very short time behavior. From Eq.(20), if we know the SPD, we can estimate the decay rate γ . However, the structure of the SPD is usually very complicated because it depends on the openness as well as the boundary geometry of the cavity. Figure 3 (a) shows the approximate of the SPD when $n = 2$ which is a snap shot of the $\tilde{P}_{sv}(s, p, t)$ captured at about $t = 12$. The partial escape property of the dielectric cavity allows for rays to distribute on unstable manifold structure in the open region, $-1/n < p < 1/n$.

Even though it is difficult to estimate the SPD in usual cases, for the large n case, the small opening case, we can simplify the SPD by assuming a uniform distribution over the whole phase space except the open regions related to the linear segments of the stadium boundary. The approximate of the SPD for $n = 10$ shown in Fig. 3 (b) supports this assumption. We note that this is a substantial difference from the escape through a small hole on boundary where entirely uniform distribution is assumed due to the ergodic property [5]. Based on the assumption of the partial ergodicity, we can rewritten the decay rate as

$$\gamma = \frac{\pi R}{\sqrt{A}(L - 2l/n)} \int dp T(p), \quad (21)$$

where we insert the factor $1/\sqrt{A}$, $A = \pi R^2 + 2Rl$ be-

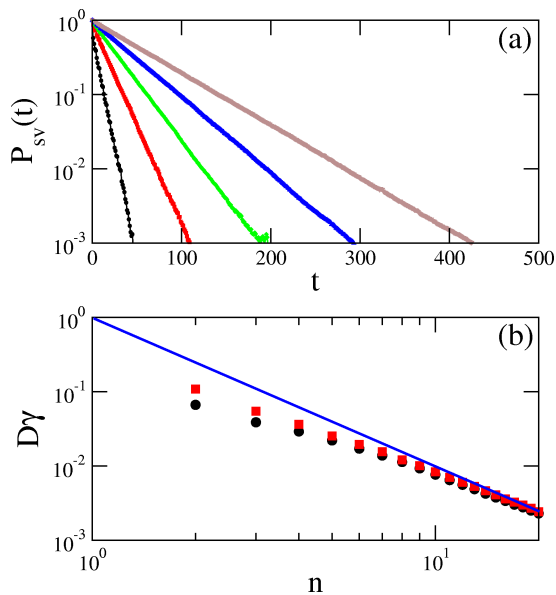


FIG. 5: (color online) The SPTD and the decay rates for TE wave. Detail of caption is the same as Fig. 4 except $D = \frac{\sqrt{AL}}{4\pi^2 R}$.

ing the area of the stadium, from the consideration of time scale. The integral of the above equation means the degree of openness and in the large n limit decreases as $\sim 2\nu\pi n^{-2}$ for both TM ($\nu = 1$) and TE ($\nu = 2$) cases (see Appendix). Therefore, for the large n limit the decay rate becomes

$$\gamma \simeq \frac{2\nu\pi^2 R}{\sqrt{AL}} n^{-2}. \quad (22)$$

Numerical results for the SPTD in the chaotic stadium-shaped dielectric cavity are shown in Figs. 4 and 5 for TM and TE cases, respectively. We take two systems; one is $(R, l) = (1, 1)$ and the other is $(R, l) = (1, 2)$. In calculation, we use a random ensemble of 10^4 initial points spread over the whole phase space and trace the survival probability with time, the time is scaled as the length of trajectory in the spatial space as before. The exponential behavior of the SPTD is clear even at long time limit in both TM and TE cases. This means that the sticky region locating on the center of the open region in phase space dose not contribute long time decay due to its easy escape. The dependence of the decay rate γ on the refractive index n shows a very good agreement with Eq.(22) for large refractive indices, in both systems with different area A . This implies that even in the small opening limit, $n \rightarrow \infty$, we cannot use the ergodic property over the whole phase space. Instead, we have to consider structure of the SPD even in the small opening limit.

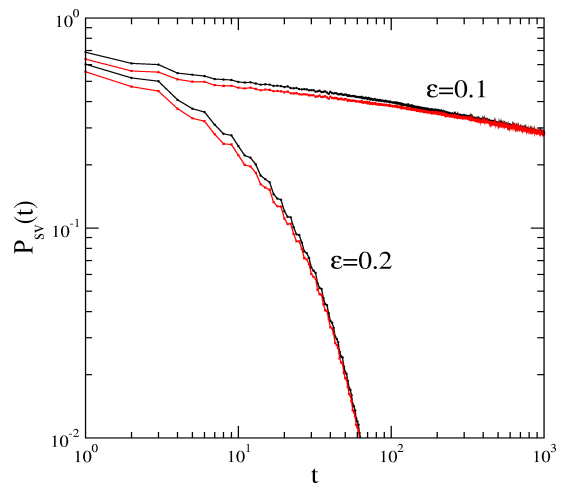


FIG. 6: (color online) The SPTDs in the quadrupolar deformed dielectric cavity. The SPTDs are algebraic in the $\varepsilon = 0.1$ cases while exponential in the $\varepsilon = 0.2$ cases. The black and red lines denote the case of TM and TE waves, respectively.

IV. QUADRUPOLE-DEFORMED DIELECTRIC CAVITY - MIXED SYSTEM

The escape property in generic mixed systems, showing a mixed phase space portrait: integrable islands in a chaotic sea, has been extensively studied. It is well known that the long time behavior of the SPTD is algebraic due to the stickiness of the KAM tori surrounding islands [11],

$$P_{sv}(t) \sim t^{-\eta}. \quad (23)$$

However, there is no rigorous theory expecting the value of the exponent η which has been estimated based on numerical calculations and seems to be nonuniversal.

In this section, we consider a quadrupolar dielectric cavity which is the typical example of a deformed microcavity and shows a mixed dynamics. The boundary equation is, in the polar coordinates,

$$r(\phi) = 1 + \varepsilon \cos 2\phi, \quad (24)$$

where ε is the deformation parameter. Here, we present numerical results of the SPTD and show that the long time behavior of the SPTD is determined by whether islands locate in the closed region, $p_c < |p| < 1$, or not.

For $n = 2$ case, we numerically calculate the SPTDs at two deformation parameter values, $\varepsilon = 0.1$ and 0.2 , which are shown in Fig. 6. In the $\varepsilon = 0.1$ case, the SPTD shows an algebraic decay, i.e., $P_{sv}(t) \sim t^{-0.2}$, which is consistent with the previous studies on mixed systems. However, in the $\varepsilon = 0.2$ case, the long time behavior of the SPTD is exponential, i.e., $P_{sv}(t) \sim \exp(-0.05t)$. This clear difference of the SPTD between $\varepsilon = 0.1$ and 0.2 cases can be explained by the phase space portraits. Figure 7 (a)

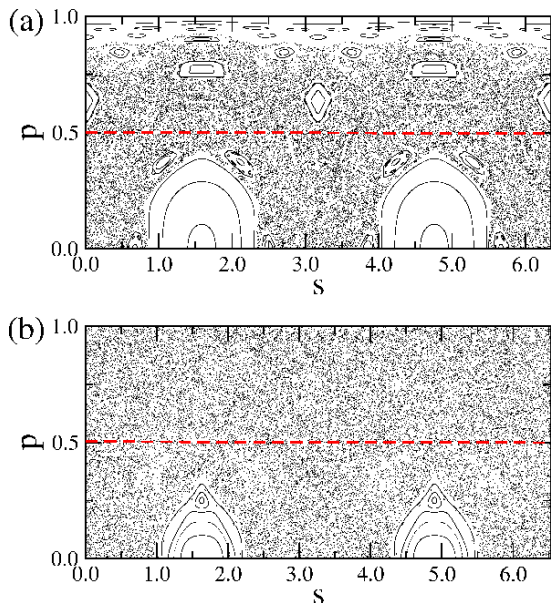


FIG. 7: The phase space portraits for the quadrupolar deformed cavity. (a) The $\varepsilon = 0.1$ case. (b) The $\varepsilon = 0.2$ case. The dashed lines denote the critical line $p_c = 1/2$ for total internal reflection for $n = 2$.

shows the phase space portrait for $\varepsilon = 0.1$ case. There are many islands in the closed region, $p_c < p < 1$, so the stickiness of the KAM tori delays the ray escape and results in the algebraic tail. On the other hand, as shown in Fig. 7 (b) there is no island in the closed region for $\varepsilon = 0.2$ case and all islands exist in the open region. The rays trapped by the stickiness of the KAM tori contribute to the short time escape behavior and the resulting SPTD shows exponential long time decay. Therefore, the position of islands plays important role to understand the SPTD of mixed systems.

V. SUMMARY

We have investigated the survival probability time distribution (SPTD) in three dielectric cavities showing different ray dynamics; circle (integrable), stadium (chaotic), quadrupole (mixed) shapes. In the circular dielectric cavity the SPTD has an algebraic long time behavior, $\sim t^{-2}$ in both TM and TE cases, but shows

very different short time behavior due to the existence of the Brewster angle in TE case where exponential short time behavior is shown. The SPTD for a stadium-shaped cavity decays exponentially, and the exponent has a close relation to the steady probability distribution (SPD). In the large n limit, the SPD can be approximated by an assumption of a partial ergodicity, a uniform distribution over a specific part of phase space, which gives a correct description of the exponent in both TM and TE cases. We have also discussed about the SPTD for the quadrupolar deformed cavity and shown that the long time behavior can be algebraic or exponential, depending on the location of islands.

Acknowledgments

This work is supported by Creative Research Initiatives of the Korean Ministry of Science and Technology.

Appendix

Here we present the analytical expression of the degree of openness (see Eq.(21)) for TM wave. The degree of openness is defined by

$$I \equiv \int_{-1/n}^{1/n} dp T(p), \quad (25)$$

where $T(p) = 1 - R(p)$, $R(p)$ is given in Eq.(2). This integral can be expressed by an analytical function as

$$\begin{aligned} I &= \frac{4}{(n^2 - 1)^2} [B(\frac{1}{2}, \frac{3}{2})F(-\frac{3}{2}, \frac{1}{2}; 2; \frac{1}{n^2})n^2 \\ &\quad + B(\frac{1}{2}, \frac{5}{2})F(-\frac{1}{2}, \frac{1}{2}; 3; \frac{1}{n^2}) - \frac{40}{15}n + \frac{8}{15} \frac{1}{n}] \\ &\simeq 2\pi n^{-2}, \end{aligned} \quad (26)$$

where $B(x, y)$ is the beta function and $F(\alpha, \beta; \gamma; z)$ the Gauss hypergeometric function [13].

For TE wave, only difference is the replacement of $R(p)$ by $R_{TE}(p)$ of Eq.(9), and the result is

$$I \simeq 4\pi n^{-2} \quad (27)$$

for the large n limit based on a numerical calculation.

-
- [1] *Optical Processes in Microcavities*, edited by R. K. Chang and A. J. Campillo (World Scientific, Singapore, 1996).
 [2] J. U. Nöckel and A. D. Stone, *Nature* **385**, 45 (1997); C. Gmachl, F. Capasso, E. E. Narimanov, J. U. Nöckel, A. D. Stone, J. Faist, D. L. Sivco, and A. Y. Cho, *Science* **280**, 1556 (1998); G. D. Chern, H. E. Tureci, A. D. Stone, R. K. Chang, M. Kneissl, and N. M. Johnson,

Appl. Phys. Lett. **83**, 1710 (2003); M. Kneissl, M. Teepe, N. Miyashita, N. M. Johnson, G. D. Chern, and R. K. Chang, *Appl. Phys. Lett.* **84**, 2485 (2004); T. Ben-Messaoud and J. Zyss, *Appl. Phys. Lett.* **86**, 241110 (2005); M. S. Kurdoglyan, S. -Y. Lee, S. Rim, and C. -M. Kim, *Opt. Lett.* **29**, 2758 (2004).

- [3] S. -Y. Lee, S. Rim, J. -W. Ryu, T. -Y. Kwon, M. Choi,

- and C. -M. Kim, Phys. Rev. Lett. **93**, 164102 (2004); S. -Y. Lee, J. -W. Ryu, T. -Y. Kwon, S. Rim, and C. -M. Kim, arXiv:nlin.CD/0505040 (2005).
- [4] *Cavity-Enhanced Spectroscopies*, edited by R. D. van Zee and J. P. Looney (Academic Press, San Diego, 2002); H. G. L. Schwefel, N. B. Rex, H. E. Tureci, R. K. Chang, A. D. Stone, T. Ben-Messaoud, and J. Zyss, J. Opt. Soc. Am. B **21**, 923 (2004).
- [5] W. Bauer and G. F. Bertsch, Phys. Rev. Lett. **65**, 2213 (1990); O. Legrand and D. Sornette, Phys. Rev. Lett. **66**, 2172 (1991); W. Bauer and G. F. Bertsh, Phys. Rev. Lett. **66**, 2173 (1991); O. Legrand and D. Sornette, Physica D **44**, 229 (1990).
- [6] E. Doron, U. Smilansky, and A. Frenkel, Phys. Rev. Lett. **65**, 3072 (1990).
- [7] N. Friedman, A. Kaplan, D. Carasso, and N. Davidson, Phys. Rev. Lett. **86**, 1518 (2001).
- [8] L. A. Bunimovich and C. P. Dettmann, Phys. Rev. Lett. **94**, 100201 (2005).
- [9] H. Alt, H. -D. Gräf, H. L. Harney, R. Hofferbert, H. Rehfeld, A. Richter, and P. Schardt, Phys. Rev. E **53**, 2217 (1996); F. Vivaldi, G. Casati, and I. Guarneri, Phys. Rev. Lett. **51**, 727 (1983); K. -C. Lee, Phys. Rev. Lett. **60**, 1991 (1988).
- [10] J. Schneider, T. Tél, and Z. Neufeld, Phys. Rev. E **66**, 066218 (2002).
- [11] A. J. Fendrik, A. M. F. Rivas, and M. J. Sánchez, Phys. Rev. E **50**, 1948 (1994); A. J. Fendrik and M. J. Sánchez, Phys. Rev. E **51**, 2996 (1995); C. F. F. Karney, Physica D **8**, 360 (1983); B. V. Chirikov and D. L. Shepelyansky, Physica D **13**, 395 (1984); P. Grassberger and H. Kantz, Phys. Lett. A **113**, 167 (1985); Y. C. Lai, M. Ding, C. Grebogi, and R. Blümel, Phys. Rev. A **46**, 4661 (1992); M. Weiss, L. Hufnagel, and R. Ketzmerick, Phys. Rev. E **67**, 046209 (2003).
- [12] J. Hawkes and I. Latimer, *Lasers; Theory and Practice* (Prentice Hall, Englewood Cliffs, NJ, 1995).
- [13] I.S. Gradshteyn, and I. M. Ryzbik, *Table of Integrals, Series, and Products*, 6th Edition (Academic Press, San Diego, 2000).